Measurement of cross sections for $e^+e^- \to \mu^+\mu^-$ at center-of-mass energies from 3.80 to 4.60 GeV

M. Ablikim,[1] M. N. Achasov,[10,e] P. Adlarson,[62] S. Ahmed,[15] M. Albrecht,[4] A. Amoroso,[61a,61c] Q. An,[58,47] Anita,[21] Y. Bai,[46] O. Bakina,[28] R. Baldini Ferroli,[23a] I. Balossino,[24a] Y. Ban,[37,m] K. Begzsuren,[26] J. V. Bennett,[5] M. Bertani,[23a] D. Bettoni,[24a] F. Bianchi,[61a,61c] J. Biernat,[62] J. Bloms,[55] A. Bortone,[61a,61c] I. Boyko,[28] R. A. Briere,[5] H. Cai,[63] X. Cai,[1,47] A. Calcaterra,[23a] G. F. Cao,[1,51] N. Cao,[1,51] S. A. Cetin,[50b] J. F. Chang,[1,47] W. L. Chang,[1,51] G. Chelkov,[28,c,d] D. Y. Chen,[6] G. Chen,[1] H. S. Chen,[1,51] M. L. Chen,[1,47] S. J. Chen,[35] X. R. Chen,[25] Y. B. Chen,[1,47] W. Cheng,[61c] G. Cibinetto,[24a] F. Cossio,[61c] X. F. Cui,[36] H. L. Dai,[1,47] J. P. Dai,[41,i] X. C. Dai,[1,51] A. Dbeyssi,[15] R. B. de Boer,[4] D. Dedovich,[28] Z. Y. Deng,[1] A. Denig,[27] I. Denysenko,[28] M. Destefanis,[61a,61c] F. De Mori,[61a,61c] Y. Ding,[33] C. Dong,[36] J. Dong,[1,47] L. Y. Dong,[1,51] M. Y. Dong,[1,47,51] S. X. Du,[66] J. Fang,[1,47] S. S. Fang,[1,51] Y. Fang,[1] R. Farinelli,[24a,24b] L. Fava,[61b,61c] F. Feldbauer,[4] G. Felici,[23a] C. Q. Feng,[58,47] M. Fritsch,[4] C. D. Fu,[1] Y. Fu,[1] X. L. Gao,[58,47] Y. Gao,[59] Y. Gao,[37,m] Y. G. Gao,[6] I. Garzia,[24a,24b] E. M. Gersabeck,[54] K. Goetzen,[11] L. Gong,[36] W. X. Gong,[1,47] W. Gradl,[27] M. Greco,[61a,61c] L. M. Gu,[35] M. H. Gu,[1,47] S. Gu,[2] Y. T. Gu,[13] C. Y. Guan,[1,51] A. Q. Guo,[22] L. B. Guo,[34] R. P. Guo,[39] Y. P. Guo,[9,j] Y. P. Guo,[27] A. Guskov,[28] S. Han,[63] T. T. Han,[40] T. Z. Han,[9,j] X. Q. Hao,[16] F. A. Harris,[52] K. L. He,[1,51] F. H. Heinsius,[4] T. Held,[4] Y. K. Heng,[1,47,51] M. Himmelreich,[11,h] T. Holtmann,[4] Y. R. Hou,[51] Z. L. Hou,[1] H. M. Hu,[1,51] J. F. Hu,[41,i] T. Hu,[1,47,51] Y. Hu,[1] G. S. Huang,[58,47] L. Q. Huang,[59] X. T. Huang,[40] Z. Huang,[37,m] N. Huesken,[55] T. Hussain,[60] W. Ikegami Andersson,[62] W. Imoehl,[22] M. Irshad,[59,47] S. Jaeger,[4] S. Janchiv,[26,l] Q. Ji,[1] Q. P. Ji,[16] X. B. Ji,[1,51] X. L. Ji,[1,47] H. B. Jiang,[40] X. S. Jiang,[1,47,51] X. Y. Jiang,[36] J. B. Jiao,[40] Z. Jiao,[18] S. Jin,[35] Y. Jin,[53] T. Johansson,[62] N. Kalantar-Nayestanaki,[30] X. S. Kang,[33] R. Kappert,[30] M. Kavatsyuk,[30] B. C. Ke,[42,1] I. K. Keshk,[4] A. Khoukaz,[55] P. Kiese,[27] R. Kiuchi,[1] R. Kliemt,[11] L. Koch,[29] O. B. Kolcu,[50b,g] B. Kopf,[4] M. Kuemmel,[4] M. Kuessner,[4] A. Kupsc,[62] M. G. Kurth,[1,51] W. Kühn,[29] J. J. Lane,[54] J. S. Lange,[29] P. Larin,[15] L. Lavezzi,[61c] H. Leithoff,[27] M. Lellmann,[27] T. Lenz,[27] C. Li,[38] C. H. Li,[32] Cheng Li,[58,47] D. M. Li,[66] F. Li,[1,47] G. Li,[1] H. B. Li,[1,51] H. J. Li,[9,j] J. L. Li,[40] J. Q. Li,[4] Ke Li,[1] L. K. Li,[1] Lei Li,[3] P. L. Li,[58,47] P. R. Li,[31] S. Y. Li,[49] W. D. Li,[1,51] W. G. Li,[1] X. H. Li,[58,47] X. L. Li,[40] Z. B. Li,[48] Z. Y. Li,[48] H. Liang,[58,47] H. Liang,[1,51] Y. F. Liang,[44] Y. T. Liang,[25] L. Z. Liao,[1,51] J. Libby,[21] C. X. Lin,[48] B. Liu,[41,i] B. J. Liu,[1] C. X. Liu,[1] D. Liu,[58,47] D. Y. Liu,[41,i] F. H. Liu,[43] Fang Liu,[1] Feng Liu,[6] H. B. Liu,[13] H. M. Liu,[1,51] Huanhuan Liu,[1] Huihui Liu,[17] J. B. Liu,[58,47] J. Y. Liu,[1,51] K. Liu,[1] K. Y. Liu,[33] Ke Liu,[6] L. Liu,[58,47] L. Y. Liu,[13] Q. Liu,[51] S. B. Liu,[58,47] T. Liu,[1,51] X. Liu,[31] Y. B. Liu,[36] Z. A. Liu,[1,47,51] Z. Q. Liu,[40] Y. F. Long,[37,m] X. C. Lou,[1,47,51] H. J. Lu,[18] J. D. Lu,[1,51] J. G. Lu,[1,47] X. L. Lu,[1] Y. Lu,[1] Y. P. Lu,[1,47] C. L. Luo,[34] M. X. Luo,[65] P. W. Luo,[48] T. Luo,[9,j] X. L. Luo,[1,47] S. Lusso,[61c] X. R. Lyu,[51] F. C. Ma,[33] H. L. Ma,[1] L. L. Ma,[40] M. M. Ma,[1,51] Q. M. Ma,[1] R. Q. Ma,[1,51] R. T. Ma,[51] X. N. Ma,[36] X. X. Ma,[1,51] X. Y. Ma,[1,47] Y. M. Ma,[40] F. E. Maas,[15] M. Maggiora,[61a,61c] S. Maldaner,[27] S. Malde,[56] Q. A. Malik,[60] A. Mangoni,[23b] Y. J. Mao,[37,m] Z. P. Mao,[1] S. Marcello,[61a,61c] Z. X. Meng,[53] J. G. Messchendorp,[30] G. Mezzadri,[24a] T. J. Min,[35] R. E. Mitchell,[22] X. H. Mo,[1,47,51] Y. J. Mo,[6] N. Yu. Muchnoi,[10,e] S. Nakhoul,[11,h] Y. Nefedov,[28] F. Nerling,[11,h] I. B. Nikolaev,[10,e] Z. Ning,[1,47] S. Nisar,[8,k] S. L. Olsen,[51] Q. Ouyang,[1,47,51] S. Pacetti,[23b] Y. Pan,[54] M. Papenbrock,[62] A. Pathak,[1] P. Patteri,[23a] M. Pelizaeus,[4] H. P. Peng,[58,47] K. Peters,[11,h] J. Pettersson,[62] J. L. Ping,[34] R. G. Ping,[1,51] A. Pitka,[4] V. Prasad,[58,47] H. Qi,[58,47] H. R. Qi,[49] M. Qi,[35] T. Y. Qi,[2] S. Qian,[1,47] W.-B. Qian,[51] C. F. Qiao,[51] L. Q. Qin,[12] X. P. Qin,[13] X. S. Qin,[4] Z. H. Qin,[1,47] J. F. Qiu,[1] S. Q. Qu,[36] K. H. Rashid,[60] K. Ravindran,[21] C. F. Redmer,[27] A. Rivetti,[61c] V. Rodin,[30] M. Rolo,[61c] G. Rong,[1,51] Ch. Rosner,[15] M. Rump,[55] A. Sarantsev,[28,f] M. Savrié,[24b] Y. Schelhaas,[27] C. Schnier,[4] K. Schoenning,[62] W. Shan,[19] X. Y. Shan,[58,47] M. Shao,[58,47] C. P. Shen,[2] P. X. Shen,[36] X. Y. Shen,[1,51] H. C. Shi,[58,47] R. S. Shi,[1,51] X. Shi,[1,47] X. D. Shi,[58,47] J. J. Song,[40] Q. Q. Song,[58,47] Y. X. Song,[37,m] S. Sosio,[61a,61c] S. Spataro,[61a,61c] F. F. Sui,[40] G. X. Sun,[1] J. F. Sun,[16] L. Sun,[63] S. S. Sun,[1,51] T. Sun,[1,51] W. Y. Sun,[34] Y. J. Sun,[58,47] Y. K. Sun,[58,47] Y. Z. Sun,[1] Z. T. Sun,[1] Y. X. Tan,[58,47] C. J. Tang,[44] G. Y. Tang,[1] J. Tang,[48] V. Thoren,[62] B. Tsednee,[26] I. Uman,[50d] B. Wang,[1] B. L. Wang,[51] C. W. Wang,[35] D. Y. Wang,[37,m] H. P. Wang,[1,51] K. Wang,[1,47] L. L. Wang,[1] M. Wang,[40] M. Z. Wang,[37,m] Meng Wang,[1,51] W. P. Wang,[58,47] X. Wang,[37,m] X. F. Wang,[31] X. L. Wang,[9,j] Y. Wang,[48] Y. Wang,[58,47] Y. D. Wang,[15] Y. F. Wang,[1,47,51] Y. Q. Wang,[1] Z. Wang,[1,47] Z. Y. Wang,[1] Ziyi Wang,[51] Zongyuan Wang,[1,51] T. Weber,[4] D. H. Wei,[12] P. Weidenkaff,[27] F. Weidner,[55] H. W. Wen,[34,a] S. P. Wen,[1] D. J. White,[54] U. Wiedner,[4] G. Wilkinson,[56] M. Wolke,[62] L. Wollenberg,[4] J. F. Wu,[1,51] L. H. Wu,[1] L. J. Wu,[1,51] X. Wu,[9,j] Z. Wu,[1,47] L. Xia,[58,47] H. Xiao,[9,j] S. Y. Xiao,[1] Y. J. Xiao,[1,51] Z. J. Xiao,[34] X. H. Xie,[37,m] Y. G. Xie,[1,47] Y. H. Xie,[6] T. Y. Xing,[1,51] X. A. Xiong,[1,51] G. F. Xu,[1] J. J. Xu,[35] Q. J. Xu,[14] W. Xu,[1,51] X. P. Xu,[45] L. Yan,[9,j] L. Yan,[61a,61c] W. B. Yan,[58,47] W. C. Yan,[66] H. J. Yang,[41,i] H. X. Yang,[1] L. Yang,[63] R. X. Yang,[58,47] S. L. Yang,[1,51] Y. H. Yang,[35] Y. X. Yang,[12] Yifan Yang,[1,51] Zhi Yang,[25] M. Ye,[1,47] M. H. Ye,[7] J. H. Yin,[1] Z. Y. You,[48] B. X. Yu,[1,47,51] C. X. Yu,[36] G. Yu,[1,51] J. S. Yu,[20,n] T. Yu,[59] C. Z. Yuan,[1,51] W. Yuan,[61a,61c] X. Q. Yuan,[37,m] Y. Yuan,[1] C. X. Yue,[32] A. Yuncu,[50b,b] A. A. Zafar,[60] Y. Zeng,[20,n] B. X. Zhang,[1] Guangyi Zhang,[16] H. H. Zhang,[48] H. Y. Zhang,[1,47] J. L. Zhang,[64] J. Q. Zhang,[4] J. W. Zhang,[1,47,51] J. Y. Zhang,[1] J. Z. Zhang,[1,51] Jianyu Zhang,[1,51] Jiawei Zhang,[1,51] L. Zhang,[1] Lei Zhang,[35] S. Zhang,[48] S. F. Zhang,[35] T. J. Zhang,[41,i] X. Y. Zhang,[40] Y. Zhang,[56]

Y. H. Zhang,[1,47] Y. T. Zhang,[58,47] Yan Zhang,[58,47] Yao Zhang,[1] Yi Zhang,[9,j] Z. H. Zhang,[6] Z. Y. Zhang,[63] G. Zhao,[1] J. Zhao,[32] J. Y. Zhao,[1,51] J. Z. Zhao,[1,47] Lei Zhao,[58,47] Ling Zhao,[1] M. G. Zhao,[36] Q. Zhao,[1] S. J. Zhao,[66] Y. B. Zhao,[1,47] Y. X. Zhao Zhao,[25] Z. G. Zhao,[58,47] A. Zhemchugov,[28,c] B. Zheng,[59] J. P. Zheng,[1,47] Y. Zheng,[37,m] Y. H. Zheng,[51] B. Zhong,[34] C. Zhong,[59] L. P. Zhou,[1,51] Q. Zhou,[1,51] X. Zhou,[63] X. K. Zhou,[51] X. R. Zhou,[58,47] A. N. Zhu,[1,51] J. Zhu,[36] K. Zhu,[1] K. J. Zhu,[1,47,51] S. H. Zhu,[57] W. J. Zhu,[36] X. L. Zhu,[49] Y. C. Zhu,[58,47] Z. A. Zhu,[1,51] B. S. Zou,[1] and J. H. Zou[1]

(BESIII Collaboration)

[1]*Institute of High Energy Physics, Beijing 100049, People's Republic of China*
[2]*Beihang University, Beijing 100191, People's Republic of China*
[3]*Beijing Institute of Petrochemical Technology, Beijing 102617, People's Republic of China*
[4]*Bochum Ruhr-University, D-44780 Bochum, Germany*
[5]*Carnegie Mellon University, Pittsburgh, Pennsylvania 15213, USA*
[6]*Central China Normal University, Wuhan 430079, People's Republic of China*
[7]*China Center of Advanced Science and Technology, Beijing 100190, People's Republic of China*
[8]*COMSATS University Islamabad, Lahore Campus, Defence Road, Off Raiwind Road, 54000 Lahore, Pakistan*
[9]*Fudan University, Shanghai 200443, People's Republic of China*
[10]*G.I. Budker Institute of Nuclear Physics SB RAS (BINP), Novosibirsk 630090, Russia*
[11]*GSI Helmholtzcentre for Heavy Ion Research GmbH, D-64291 Darmstadt, Germany*
[12]*Guangxi Normal University, Guilin 541004, People's Republic of China*
[13]*Guangxi University, Nanning 530004, People's Republic of China*
[14]*Hangzhou Normal University, Hangzhou 310036, People's Republic of China*
[15]*Helmholtz Institute Mainz, Johann-Joachim-Becher-Weg 45, D-55099 Mainz, Germany*
[16]*Henan Normal University, Xinxiang 453007, People's Republic of China*
[17]*Henan University of Science and Technology, Luoyang 471003, People's Republic of China*
[18]*Huangshan College, Huangshan 245000, People's Republic of China*
[19]*Hunan Normal University, Changsha 410081, People's Republic of China*
[20]*Hunan University, Changsha 410082, People's Republic of China*
[21]*Indian Institute of Technology Madras, Chennai 600036, India*
[22]*Indiana University, Bloomington, Indiana 47405, USA*
[23a]*INFN Laboratori Nazionali di Frascati, I-00044 Frascati, Italy*
[23b]*INFN and University of Perugia, I-06100 Perugia, Italy*
[24a]*INFN Sezione di Ferrara, I-44122 Ferrara, Italy*
[24b]*University of Ferrara, I-44122 Ferrara, Italy*
[25]*Institute of Modern Physics, Lanzhou 730000, People's Republic of China*
[26]*Institute of Physics and Technology, Peace Ave. 54B, Ulaanbaatar 13330, Mongolia*
[27]*Johannes Gutenberg University of Mainz, Johann-Joachim-Becher-Weg 45, D-55099 Mainz, Germany*
[28]*Joint Institute for Nuclear Research, 141980 Dubna, Moscow Region, Russia*
[29]*Justus-Liebig-Universitaet Giessen, II. Physikalisches Institut, Heinrich-Buff-Ring 16, D-35392 Giessen, Germany*
[30]*KVI-CART, University of Groningen, NL-9747 AA Groningen, Netherlands*
[31]*Lanzhou University, Lanzhou 730000, People's Republic of China*
[32]*Liaoning Normal University, Dalian 116029, People's Republic of China*
[33]*Liaoning University, Shenyang 110036, People's Republic of China*
[34]*Nanjing Normal University, Nanjing 210023, People's Republic of China*
[35]*Nanjing University, Nanjing 210093, People's Republic of China*
[36]*Nankai University, Tianjin 300071, People's Republic of China*
[37]*Peking University, Beijing 100871, People's Republic of China*
[38]*Qufu Normal University, Qufu 273165, People's Republic of China*
[39]*Shandong Normal University, Jinan 250014, People's Republic of China*
[40]*Shandong University, Jinan 250100, People's Republic of China*
[41]*Shanghai Jiao Tong University, Shanghai 200240, People's Republic of China*
[42]*Shanxi Normal University, Linfen 041004, People's Republic of China*
[43]*Shanxi University, Taiyuan 030006, People's Republic of China*
[44]*Sichuan University, Chengdu 610064, People's Republic of China*
[45]*Soochow University, Suzhou 215006, People's Republic of China*
[46]*Southeast University, Nanjing 211100, People's Republic of China*

[47]*State Key Laboratory of Particle Detection and Electronics, Beijing 100049, Hefei 230026, People's Republic of China*
[48]*Sun Yat-Sen University, Guangzhou 510275, People's Republic of China*
[49]*Tsinghua University, Beijing 100084, People's Republic of China*
[50a]*Ankara University, 06100 Tandogan, Ankara, Turkey*
[50b]*Istanbul Bilgi University, 34060 Eyup, Istanbul, Turkey*
[50c]*Uludag University, 16059 Bursa, Turkey*
[50d]*Near East University, Nicosia, North Cyprus, Mersin 10, Turkey*
[51]*University of Chinese Academy of Sciences, Beijing 100049, People's Republic of China*
[52]*University of Hawaii, Honolulu, Hawaii 96822, USA*
[53]*University of Jinan, Jinan 250022, People's Republic of China*
[54]*University of Manchester, Oxford Road, Manchester M13 9PL, United Kingdom*
[55]*University of Muenster, Wilhelm-Klemm-Str. 9, 48149 Muenster, Germany*
[56]*University of Oxford, Keble Rd, Oxford OX13RH, United Kingdom*
[57]*University of Science and Technology Liaoning, Anshan 114051, People's Republic of China*
[58]*University of Science and Technology of China, Hefei 230026, People's Republic of China*
[59]*University of South China, Hengyang 421001, People's Republic of China*
[60]*University of the Punjab, Lahore-54590, Pakistan*
[61a]*University of Turin, I-10125 Turin, Italy*
[61b]*University of Eastern Piedmont, I-15121 Alessandria, Italy*
[61c]*INFN, I-10125 Turin, Italy*
[62]*Uppsala University, Box 516, SE-75120 Uppsala, Sweden*
[63]*Wuhan University, Wuhan 430072, People's Republic of China*
[64]*Xinyang Normal University, Xinyang 464000, People's Republic of China*
[65]*Zhejiang University, Hangzhou 310027, People's Republic of China*
[66]*Zhengzhou University, Zhengzhou 450001, People's Republic of China*

(Received 26 July 2020; accepted 9 November 2020; published 16 December 2020)

The observed cross sections for $e^+e^- \to \mu^+\mu^-$ at energies from 3.8 to 4.6 GeV are measured using data samples taken with the BESIII detector operated at the BEPCII collider. We measure the muonic widths and determine the branching fractions of the charmonium states $\psi(4040)$, $\psi(4160)$, and $\psi(4415)$ decaying to $\mu^+\mu^-$, as well as making a first determination of the phase of the amplitudes. In addition, we observe evidence for a structure in the dimuon cross section near 4.220 GeV/c^2, which we denote as $S(4220)$. Analyzing a coherent sum of amplitudes yields eight solutions, one of which gives a mass of $M_{S(4220)} = 4216.7 \pm 8.9 \pm 4.1$ MeV/c^2, a total width of $\Gamma^{\rm tot}_{S(4220)} = 47.2 \pm 22.8 \pm 10.5$ MeV, and a muonic width of $\Gamma^{\mu\mu}_{S(4220)} = 1.53 \pm 1.26 \pm 0.54$ keV, where the first uncertainties are statistical and the second systematic. The eight solutions give the central values of the mass, total width, muonic width to be,

[a]Also at Ankara University, 06100 Tandogan, Ankara, Turkey.
[b]Also at Bogazici University, 34342 Istanbul, Turkey.
[c]Also at the Moscow Institute of Physics and Technology, Moscow 141700, Russia.
[d]Also at the Functional Electronics Laboratory, Tomsk State University, Tomsk 634050, Russia.
[e]Also at the Novosibirsk State University, Novosibirsk 630090, Russia.
[f]Also at the NRC "Kurchatov Institute", PNPI, 188300, Gatchina, Russia.
[g]Also at Istanbul Arel University, 34295 Istanbul, Turkey.
[h]Also at Goethe University Frankfurt, 60323 Frankfurt am Main, Germany.
[i]Also at Key Laboratory for Particle Physics, Astrophysics and Cosmology, Ministry of Education; Shanghai Key Laboratory for Particle Physics and Cosmology; Institute of Nuclear and Particle Physics, Shanghai 200240, People's Republic of China.
[j]Also at Key Laboratory of Nuclear Physics and Ion-beam Application (MOE) and Institute of Modern Physics, Fudan University, Shanghai 200443, People's Republic of China.
[k]Also at Harvard University, Department of Physics, Cambridge, Massachusetts 02138, USA.
[l]Currently at: Institute of Physics and Technology, Peace Ave.54B, Ulaanbaatar 13330, Mongolia.
[m]Also at State Key Laboratory of Nuclear Physics and Technology, Peking University, Beijing 100871, People's Republic of China.
[n]School of Physics and Electronics, Hunan University, Changsha 410082, China.

respectively, in the range from 4212.8 to 4219.4 MeV/c^2, from 36.4 to 49.6 MeV, and from 1.09 to 1.53 keV. The statistical significance of the $S(4220)$ signal is 3.9σ. Correcting the total dimuon cross section for radiative effects yields a statistical significance for this structure of 8.1σ.

DOI: 10.1103/PhysRevD.102.112009

For a long time the meson resonances produced in e^+e^- collisions above the open-charm (OC) and below the open-bottom thresholds had been thought to decay entirely to OC final states through the strong interaction. Consequently, the possibility of nonopen-charm (NOC) decays attracted little experimental interest until the early years of the millennium. For convenience, in this paper we denote these resonances $X_{\text{above D}\bar{\text{D}}}$, which encompasses both heavy $c\bar{c}$ states, i.e., $\psi(3770)$, $\psi(4040)$, $\psi(4160)$, and $\psi(4415)$, and non-$c\bar{c}$ states, such as four-quark composites, hybrid charmonium states, and open-charm molecule states [1–3] that are expected by QCD. Finding these non-$c\bar{c}$ states would be a crucial validation of the QCD predictions.

Since non-$c\bar{c}$ states may easily decay to NOC final states, such decays of $X_{\text{above D}\bar{\text{D}}}$ mesons were searched for by the BES collaboration using the data collected with the BES-I detector at energies of 4.04 and 4.14 GeV, and the BES-II detector at energies around 3.773 GeV. The first evidence for such decays was reported in the $J/\psi\pi^+\pi^-$ final state by BES in 2003 [4]. This final state could come from the decay of a $c\bar{c}$ or a non-$c\bar{c}$ state, or even both of these states. On the assumption that there is no other resonance at energies near 3.773 GeV, the signal was interpreted to be $\psi(3770) \to J/\psi\pi^+\pi^-$ [5]. This first NOC decay was confirmed by the CLEO collaboration [6] two year after the BES analysis. This discovery overturned the conventional understanding that $X_{\text{above D}\bar{\text{D}}}$ decay into OC final states through the strong interaction with branching fractions of almost 100%. It stimulated strong interest in searching for other NOC decays of $X_{\text{above D}\bar{\text{D}}}$ mesons [7], in particular into $J/\psi\pi^+\pi^-$ and similar final states, and led to the discovery of several new resonances [8–10].

In the last 17 years, several new states [8–10], and new di-structures, such as the $Rs(3770)$ [11] and $R(4220)$ and $R(4320)$ [12], as well as structures lying above 4.2 GeV [13,14] have been observed in e^+e^- annihilation at energies above the OC threshold. The $X(3872)$ [8], $Y(4260)$ [9], and $R(4220)$ and $R(4320)$ [12] resonances were observed in the $J/\psi\pi^+\pi^-$ final state, while the $Y(4360)$ [10] and $Y(4660)$ [10] were observed in the $\psi(3686)\pi^+\pi^-$ final state. In addition, the $Y(4220)$ [13] was observed in the final state $\omega\chi_{c0}$, and the $Y(4220)$ and $Y(4390)$ [12] were observed in the final state $h_c\pi^+\pi^-$. All of these resonances were observed in final states of inclusive hadrons, where no attempt was made to identify the hadron species, and in final states of $M_{c\bar{c}}X_{\text{LH}}$, where $M_{c\bar{c}}$ is a hidden-charm meson and X_{LH} is a light hadron.

In searching for new states, as suggested in Ref. [15], lineshape of cross sections for $e^+e^- \to J/\psi X$ and $e^+e^- \to \psi(3686)X$ ($X =$ light hadrons or photons) are studied by BESIII. In addition, searches for new vector states could be also performed by analyzing the cross section of $e^+e^- \to \mu^+\mu^-$. Although the dimuon branching fractions of the $X_{\text{above D}\bar{\text{D}}}$ decays are all at or less than the level of $\sim 10^{-5}$, the interference of these decays with $e^+e^- \to \mu^+\mu^-$ continuum processes could produce a measurable contribution to the cross section, and make the $X_{\text{above D}\bar{\text{D}}}$ states seeable.

In this Letter, we report measurements of the cross section for $e^+e^- \to \mu^+\mu^-$ at center-of-mass (c.m.) energies from 3.8 to 4.6 GeV, and studies of the known $c\bar{c}$ resonances and searches for new structures in this regime by performing an analysis of a coherent sum of amplitudes contributing of this cross section. The data samples used in measuring the cross section were collected at 133 c.m. energies with the BESIII detector operated at the BEPCII collider from 2011 to 2017. The total integrated luminosity of the data sets used in the analysis is 13.2 fb^{-1}, determined from large-angle Bhabha scattering events [16]. The c.m. energy of each data set is measured using dimuon events, with an uncertainty of ± 0.8 MeV [17].

The BESIII detector is described in detail in Ref. [18]. The detector response is studied using samples of Monte Carlo (MC) events which are simulated with the GEANT4-based [19] detector simulation software package BOOST. Simulated samples for all vector $q\bar{q}$ states (i.e., $u\bar{u}$, $d\bar{d}$, $s\bar{s}$, and $c\bar{c}$ resonances) and their decays to $\mu^+\mu^-$ are generated with the MC event generator BABAYAGA [20]. Possible background sources are estimated with Monte Carlo simulated events generated with the event generator KKMC [21]. The detection efficiency is determined with Monte Carlo simulated $e^+e^- \to \mu^+\mu^-$ events generated with BABAYAGA, which includes initial and final state radiation, as well as vacuum polarization effects.

The observed cross section for $e^+e^- \to \mu^+\mu^-$ at a certain c.m. energy $\sqrt{s}$ is determined by

$$\sigma^{\text{obs}}(e^+e^- \to \mu^+\mu^-) = \frac{N^{\text{obs}}}{\mathcal{L}\epsilon}, \tag{1}$$

where N^{obs} is the background-subtracted number of observed events for $e^+e^- \to \mu^+\mu^-$, $\mathcal{L}$ is the integrated luminosity, and ϵ is the detection efficiency.

Each candidate for $e^+e^- \to \mu^+\mu^-$ is required to have two tracks of opposite charge. Each of the two charged tracks

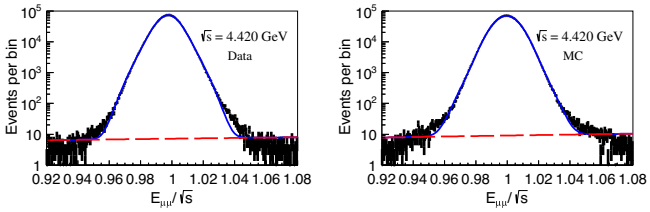

FIG. 1. Distributions of the ratios of the total energies $E_{\mu^+\mu^-}$ of the $\mu^+\mu^-$ system to $\sqrt{s}$ for the events selected from the data (left) collected at $\sqrt{s} = 4.42$ GeV and MC events (right) simulated at the same energy. The black dots with error bars show the data and MC events, the blue solid line shows the fit to these, and the red dashed line shows the backgrounds.

must satisfy $|\cos\theta| < 0.8$, where θ is the polar angle of the tracks. In addition, the charged tracks are required to satisfy $V_r < 1.0$ cm and $|V_z| < 10.0$ cm, where V_r is the distance of closest approach to the interaction point in the r-ϕ plane, and $|V_z|$ is the distance between the point of the closest approach and the interaction point along the beam axis. Furthermore, the total momentum $|\vec{p}_+| + |\vec{p}_-|$ of the two charged tracks is required to be greater than 90% of the nominal collision energy $\sqrt{s}$. To reject Bhabha scattering events, we require the ratio of the energy $E_\pm$ deposited in the electromagnetic calorimeter to the momentum $p_\pm$ of the charged track to satisfy $0.05 < E_\pm/p_\pm < 0.40$. This criterion also rejects $\pi^+\pi^-$ pairs. The rejection fraction for $\pi^+\pi^-$ events is energy dependent, ranging from 41.5% at 3.8 GeV to 37.5% at 4.6 GeV. The remaining $\pi^+\pi^-$ background is subtracted using the extrapolation of the $e^+e^- \to \pi^+\pi^-$ cross section measured by the CLEO collaboration [22] and the rate of misidentifying $\pi^+\pi^-$ as $\mu^+\mu^-$ obtained from the MC simulation. In order to reduce the K^+K^- and $p\bar{p}$ background, the event is subjected to a four-constraint kinematic fit with the hypothesis $e^+e^- \to \mu^+\mu^-$, constraining the total four-momentum of the $\mu^+\mu^-$ to that of the colliding beams, and the fit $\chi^2_{\rm 4C}$ is required to be less than 60.

The number of $e^+e^- \to \mu^+\mu^-$ candidates is determined by analyzing the ratio $E_{\mu^+\mu^-}/\sqrt{s}$, where $E_{\mu^+\mu^-}$ is the total energy of μ^+ and μ^- determined from the measured track momenta. As an example, Fig. 1 (left) shows the distribution of $E_{\mu^+\mu^-}/\sqrt{s}$ for the events selected from the data collected at $\sqrt{s} = 4.420$ GeV. A fit to the distribution with a double-Gaussian function for the signal shape and a first order polynomial to describe the background yields $N^{\rm fit} = (2500.2 \pm 1.6) \times 10^3$ $e^+e^- \to \mu^+\mu^-$ candidates, where the uncertainty is statistical. The systematic uncertainty due to the nonpeaking background (mainly cosmic rays and beam-gas events) is estimated to be less than 0.01%, and therefore negligible. The imperfection of the signal peak description is taken into account as a systematic uncertainty (see below). The signal yield $N^{\rm fit}$ is still contaminated by peaking background from several sources, e.g., $e^+e^- \to (\gamma)e^+e^-$, $e^+e^- \to \pi^+\pi^-$, and $e^+e^- \to K^+K^-$. Using the high-statistics samples of MC simulated events and the extrapolated cross sections for these processes, the number of the background events is estimated to be $N^{\rm b} = 4764 \pm 18$, where the uncertainty is mostly due to the cross-section extrapolation. Subtracting $N^{\rm b}$ from $N^{\rm fit}$ yields $N^{\rm obs} = (2495.4 \pm 1.6) \times 10^3$ signal events.

The integrated luminosity of the data sample taken at 4.420 GeV was previously measured to be $\mathcal{L} = 1043.9 \pm 0.1 \pm 6.9$ pb^{-1} [16], where the first uncertainty is statistical and the second one is systematic. At 4.420 GeV, the detection efficiency of $e^+e^- \to \mu^+\mu^-$ is $\epsilon = (41.09 \pm 0.01)\%$, as determined from the MC. Using these values in Eq. (1) yields the observed cross section of $\sigma^{\rm obs}(e^+e^- \to \mu^+\mu^-) = 5.818 \pm 0.010 \pm 0.169$ nb. The first error includes the uncertainties of statistical origin (signal sample size, MC event statistics and the statistical uncertainty of the luminosity measurement). The second error represents the remaining systematic uncertainties (see below). Similarly, we determine the observed cross sections for $e^+e^- \to \mu^+\mu^-$ at the other 132 energies from 3.81 to 4.6 GeV.

The systematic uncertainty for the observed cross section originates from several sources. They are 1% due to the luminosity measurement, 1% per track associated with the knowledge of the tracking efficiency, 0.64% due to requiring $|\cos\theta| < 0.8$, 0.59% due to requiring $|\vec{p}_+| + |\vec{p}_-| > 0.9\sqrt{s}$, 0.12% due to the selection on $E_\pm/|\vec{p}_\pm|$, 0.41% due to the four-constraint kinematic fit, 1.23% due to the fit to the $E_{\mu^+\mu^-}/\sqrt{s}$ distribution, 0.03% due to the background subtraction, and 1% due to the theoretical uncertainty associated with the Monte Carlo generator. An additional uncertainty arises from the imperfect description of the signal shape by the fit (see Fig. 1). This effect is only partially compensated by the MC, and the residual uncertainty is 0.03%. Adding these uncertainties in quadrature yields a total systematic uncertainty of 2.91%.

To search for new vector states in $e^+e^- \to \mu^+\mu^-$, a χ^2 fit is performed to the measured cross section. In the fit, the expected cross section is given by [23,24]

$$\sigma^{\rm exp}_{\mu^+\mu^-}(s) = \int_0^{1-\frac{4m_\mu^2}{s}} dx \cdot \sigma^{\rm D}_{\mu^+\mu^-}(s(1-x))F(x,s), \quad (2)$$

where m_μ is the mass of muon and $F(x,s)$ is a sampling function [25] for the radiative photon energy fraction x. $\sigma^{\rm D}(s(1-x))$ is the dressed cross section including vacuum-polarization effects,

$$\sigma^{\rm D}_{\mu^+\mu^-}(s(1-x)) = \left| A_{\rm cnt} + \sum_{k=1}^{9} e^{i\phi_{R_k}} A_{R_k} + e^{i\phi_S} A_S \right|^2 \quad (3)$$

where $A_{\rm cnt}$, A_{R_k} and $A_{\rm S}$ are, respectively, the amplitude for continuum $e^+e^- \to \mu^+\mu^-$ production, the Breit-Wigner

(BW) amplitude describing nine vector resonances ($\rho(770)$, $\omega(782)$, $\phi(1020)$, J/ψ, $\psi(3686)$, $\psi(3770)$, $\psi(4040)$, $\psi(4160)$, and $\psi(4415)$), and a new vector structure S decaying into $\mu^+\mu^-$, while ϕ_{R_k} and ϕ_S are the corresponding phases of the amplitudes. The continuum amplitude can be parameterized as $A_{\rm cnt} = \sqrt{f_{\rm cnt}/s'}$, where $f_{\rm cnt}$ is a free parameter, and $s' = s(1-x)$. The decay amplitude of resonance $\mathcal{R}$, being either one of the known vector states or the new structure S, is written as $\mathcal{A} = \sqrt{12\pi\Gamma^{ee}_{\mathcal{R}}\Gamma^{\mu\mu}_{\mathcal{R}}}/[(s' - M^2_{\mathcal{R}}) + i\Gamma^{\rm tot}_{\mathcal{R}}M_{\mathcal{R}}]$, where $M_{\mathcal{R}}$, $\Gamma^{ee}_{\mathcal{R}}$, $\Gamma^{\mu\mu}_{\mathcal{R}}$ and $\Gamma^{\rm tot}_{\mathcal{R}}$ are the mass, electron width, muonic width, and total width, respectively.

In the fit the observed cross section values are assumed to be influenced only by the uncertainties of statistical origin. The uncertainties on the parameters returned by the fit are referred to as statistical uncertainties in the subsequent discussion. The remaining cross section uncertainties (assumed to be fully correlated between different energies) are taken into account using the "offset method" [26]: the cross-section values are changed for all energies simultaneously by the size of the uncertainty and the resulting change in the fit parameter is taken as a systematic uncertainty.

Since the analysis does not include the observed cross section at energies below 3.8 GeV, the parameters of the first six lower mass vector resonances are all fixed to the values given by the particle data group (PDG) [27], whose phase corresponds to zero. For the three heavy $c\bar{c}$ states, i.e., $\psi(4040)$, $\psi(4160)$, and $\psi(4415)$, the masses and the total widths are also fixed to the values given by the PDG. The partial widths $\Gamma^{\mu\mu}$ and the phases are left free, and lepton universality is assumed (i.e., $\Gamma^{ee}_{\mathcal{R}} = \Gamma^{\mu\mu}_{\mathcal{R}}$). It is noted that the earlier studies contributing to the values for $\Gamma^{ee}_{\mathcal{R}}$ reported in Ref. [27] did not consider the contributions from non-$c\bar{c}$ states in the calculations of the initial state radiative (ISR) correction factors; furthermore they assumed a selection efficiency for $e^+e^- \to$ hadrons that is a smooth curve, increasing as the c.m. energy increases, rather than the BW-like function observed in e.g., Fig. 1(b) of Ref. [28]. Neglecting these effects may lead to bias, as may the difficulties of accounting for interference effects between the continuum $e^+e^- \to$ hadrons amplitude and the resonance decay amplitudes. Following these considerations we leave these partial widths as free parameters in our fit.

The fit returns eight acceptable solutions with distinct results for the four free phases. Table I shows the results from the fit. All solutions include a result for a new structure with mass close to 4220 MeV, and so we denote this possible state as $S(4220)$. For Solution I, the fit returns $f_{\rm cnt} = 88.51 \pm 0.11$ nb/GeV^2 and $\chi^2 = 135.47$ for 121 degrees of freedom. Taking $\Gamma^{\mu\mu}_{S(4220)} = \Gamma^{\rm tot}_{S(4220)}\mathcal{B}(S(4220)\to\mu^+\mu^-)$, where $\mathcal{B}(S(4220)\to\mu^+\mu^-)$ is the branching fraction for the decay of $S(4220) \to \mu^+\mu^-$, the fit yields $\Gamma^{ee}_{S(4220)}\mathcal{B}(S(4220) \to \mu^+\mu^-) = 0.05 \pm 0.06 \pm 0.03$ eV, where the first uncertainty is statistical and the second is systematic.

Figure 2 (left) shows the observed cross sections with a fit to the sum of eleven contributions: continuum $e^+e^- \to \mu^+\mu^-$, the nine known vector states and the $S(4220)$ decay into $\mu^+\mu^-$. The black empty circles in Fig. 2 are for the lower luminosity data (integrated luminosity less than 12 pb^{-1}), the filled red circles are for the higher luminosity data, the solid line is for the fit, and the dashed line is for the contribution from the $e^+e^- \to \mu^+\mu^-$ continuum. Figure 2 (right) shows the corresponding observed cross section, for which both the contributions from the continuum $e^+e^- \to \mu^+\mu^-$ and the decay $\psi(3686) \to \mu^+\mu^-$ are subtracted. Removing the $S(4220)$ from the fit yields a χ^2 change by 23.78, for a reduction of four degrees of freedom, which corresponds to a statistical significance for the structure of 3.9σ.

The systematic uncertainties on the values of the parameters given in Table I originate from three sources: (1) systematic uncertainties on the observed cross sections, (2) uncertainties on the parameters for the $\psi(3686)$, $\psi(3770)$, $\psi(4040)$, $\psi(4160)$, and $\psi(4415)$ states, (3) uncertainties on the c.m. energies. Adding these contributions in quadrature we obtain the total systematic uncertainties for the fit parameters, which are listed as the second uncertainties in Table I.

Initial state radiation distorts the shape of the resonances in the observed cross section. Most ISR events not only populate the valleys between the resonance peaks [see cross section around 4.02, 4.20, and 4.36 GeV in Fig. 2 (right)], but also reduce the heights of these peaks, which weakens the significance of the signals. Figure 3 (left) shows the corresponding Born-continuum-dressed-resonance (BCDR) cross section, which is the observed cross section divided by the ISR correction factor $f_{\rm ISR}(s)$, with $f_{\rm ISR}(s) = \sigma^{\rm obs}_{\mu^+\mu^-}(s)/\sigma^{\rm D}_{\mu^+\mu^-}(s)$, where $\sigma^{\rm obs}_{\mu^+\mu^-}(s)$ is given in Eq. (2) and $\sigma^{\rm D}_{\mu^+\mu^-}(s)$ is given in Eq. (3) with $x = 0$. The BCDR cross section is the sum of the Born continuum cross section of $e^+e^- \to \mu^+\mu^-$ and the dressed cross sections for the resonances decaying into $\mu^+\mu^-$. The ISR correction removes the ISR-return events [see cross section around 4.02, 4.20, and 4.36 GeV in Fig. 3 (right)] and restores the heights of the signal peaks, making the $S(4220)$ signal to be more pronounced and more clearly seen in the BCDR cross sections. Removing the $S(4220)$ from the fit to the BCDR cross section causes a χ^2 change by 78.20, for a reduction of four degrees of freedom. This change corresponds to a statistical significance of $(8.13 \pm 0.06)\sigma$ for the $S(4220)$ structure, where the uncertainty is due to the uncertainties of the fixed parameter values of $\psi(3770)$, $\psi(4040)$, $\psi(4160)$ and $\psi(4415)$ resonances in calculation of ISR correction factors. Analysis of an ensemble of simulated data sets of $e^+e^- \to h_c\pi^+\pi^-$ generated using the Y(4220) and Y(4390) resonance parameters [14] demonstrates that the signal significance of

TABLE I. Results from the fit to the $e^+e^- \to \mu^+\mu^-$ cross section showing the values of the muonic width $\Gamma^{\mu\mu}_{\mathcal{R}_i}$ [in keV], branching fraction $\mathcal{B}(\mathcal{R}_i \to \mu^+\mu^-)$ [10^{-5}] and phase $\phi_{\mathcal{R}_i}$ [in degree], where $\mathcal{R}_1$, $\mathcal{R}_2$, $\mathcal{R}_3$ and $\mathcal{R}_4$ represent $\psi(4040)$, $\psi(4160)$, $\psi(4415)$ and $S(4220)$, respectively. Also given is the mass $M_{\mathcal{R}_4}$ [in MeV], and total width $\Gamma^{\rm tot}_{\mathcal{R}_4}$ [in MeV] of the $S(4220)$. The first uncertainties are statistical, and the second are systematic.

Parameters	Solution I	Solution II	Solution III	Solution IV
$\Gamma^{\mu\mu}_{\mathcal{R}_1}$	$0.73 \pm 0.48 \pm 0.12$	$0.62 \pm 0.46 \pm 0.10$	$0.58 \pm 0.52 \pm 0.10$	$0.71 \pm 0.42 \pm 0.12$
$\mathcal{B}(\mathcal{R}_1 \to \mu^+\mu^-)$	$0.91 \pm 0.60 \pm 0.20$	$0.77 \pm 0.58 \pm 0.17$	$0.72 \pm 0.65 \pm 0.15$	$0.89 \pm 0.53 \pm 0.19$
$\phi_{\mathcal{R}_1}$	$283 \pm 33 \pm 40$	$285 \pm 38 \pm 41$	$286 \pm 37 \pm 41$	$283 \pm 39 \pm 40$
$\Gamma^{\mu\mu}_{\mathcal{R}_2}$	$2.45 \pm 1.24 \pm 0.94$	$2.36 \pm 1.26 \pm 0.91$	$2.28 \pm 0.82 \pm 0.88$	$2.41 \pm 1.08 \pm 0.93$
$\mathcal{B}(\mathcal{R}_2 \to \mu^+\mu^-)$	$3.49 \pm 1.78 \pm 1.22$	$3.37 \pm 1.80 \pm 1.18$	$3.26 \pm 1.16 \pm 1.15$	$3.45 \pm 1.54 \pm 1.21$
$\phi_{\mathcal{R}_2}$	$153 \pm 33 \pm 11$	$138 \pm 29 \pm 10$	$136 \pm 26 \pm 10$	$150 \pm 11 \pm 11$
$\Gamma^{\mu\mu}_{\mathcal{R}_3}$	$1.25 \pm 0.28 \pm 0.35$	$1.26 \pm 0.27 \pm 0.35$	$1.27 \pm 0.41 \pm 0.36$	$1.24 \pm 0.27 \pm 0.35$
$\mathcal{B}(\mathcal{R}_3 \to \mu^+\mu^-)$	$2.01 \pm 0.44 \pm 0.87$	$2.03 \pm 0.44 \pm 0.88$	$2.05 \pm 0.66 \pm 0.89$	$2.01 \pm 0.44 \pm 0.87$
$\phi_{\mathcal{R}_3}$	$334 \pm 13 \pm 128$	$332 \pm 13 \pm 130$	$332 \pm 13 \pm 130$	$333 \pm 12 \pm 136$
$M_{\mathcal{R}_4}$	$4216.7 \pm 8.9 \pm 4.1$	$4213.6 \pm 7.5 \pm 4.1$	$4213.7 \pm 6.0 \pm 4.1$	$4216.2 \pm 5.7 \pm 4.1$
$\Gamma^{\rm tot}_{\mathcal{R}_4}$	$47.2 \pm 22.8 \pm 10.5$	$39.9 \pm 19.5 \pm 8.9$	$38.5 \pm 12.8 \pm 8.5$	$45.5 \pm 13.3 \pm 10.1$
$\Gamma^{\mu\mu}_{\mathcal{R}_4}$	$1.53 \pm 1.26 \pm 0.54$	$1.28 \pm 1.09 \pm 0.46$	$1.20 \pm 0.67 \pm 0.42$	$1.46 \pm 0.89 \pm 0.52$
$\phi_{\mathcal{R}_4}$	$20 \pm 44 \pm 13$	$0 \pm 40 \pm 0$	$359 \pm 33 \pm 180$	$17 \pm 19 \pm 11$
Parameters	Solution V	Solution VI	Solution VII	Solution VIII
$\Gamma^{\mu\mu}_{\mathcal{R}_1}$	$0.74 \pm 0.50 \pm 0.12$	$0.58 \pm 0.46 \pm 0.10$	$0.66 \pm 0.46 \pm 0.11$	$0.80 \pm 0.48 \pm 0.13$
$\mathcal{B}(\mathcal{R}_1 \to \mu^+\mu^-)$	$0.93 \pm 0.63 \pm 0.20$	$0.72 \pm 0.57 \pm 0.16$	$0.83 \pm 0.58 \pm 0.18$	$1.00 \pm 0.60 \pm 0.22$
$\phi_{\mathcal{R}_1}$	$282 \pm 31 \pm 40$	$287 \pm 41 \pm 39$	$291 \pm 37 \pm 42$	$284 \pm 30 \pm 40$
$\Gamma^{\mu\mu}_{\mathcal{R}_2}$	$2.28 \pm 1.05 \pm 0.88$	$2.22 \pm 1.12 \pm 0.85$	$2.08 \pm 0.99 \pm 0.80$	$2.31 \pm 1.14 \pm 0.89$
$\mathcal{B}(\mathcal{R}_2 \to \mu^+\mu^-)$	$3.26 \pm 1.46 \pm 1.14$	$3.17 \pm 1.61 \pm 1.11$	$2.97 \pm 1.41 \pm 1.04$	$3.29 \pm 1.63 \pm 1.15$
$\phi_{\mathcal{R}_2}$	$157 \pm 37 \pm 12$	$132 \pm 28 \pm 10$	$143 \pm 29 \pm 11$	$154 \pm 31 \pm 12$
$\Gamma^{\mu\mu}_{\mathcal{R}_3}$	$1.24 \pm 0.28 \pm 0.35$	$1.27 \pm 0.27 \pm 0.36$	$1.24 \pm 0.27 \pm 0.35$	$1.25 \pm 0.27 \pm 0.35$
$\mathcal{B}(\mathcal{R}_3 \to \mu^+\mu^-)$	$2.00 \pm 0.45 \pm 0.87$	$2.05 \pm 0.43 \pm 0.89$	$2.01 \pm 0.43 \pm 0.87$	$2.02 \pm 0.44 \pm 0.87$
$\phi_{\mathcal{R}_3}$	$335 \pm 13 \pm 135$	$331 \pm 12 \pm 126$	$332 \pm 13 \pm 130$	$332 \pm 13 \pm 132$
$M_{\mathcal{R}_4}$	$4219.4 \pm 11.2 \pm 4.1$	$4212.8 \pm 7.2 \pm 4.0$	$4216.1 \pm 7.5 \pm 4.1$	$4217.3 \pm 9.1 \pm 4.1$
$\Gamma^{\rm tot}_{\mathcal{R}_4}$	$49.6 \pm 22.6 \pm 11.0$	$36.4 \pm 16.8 \pm 8.1$	$37.8 \pm 18.5 \pm 8.4$	$45.5 \pm 21.2 \pm 10.1$
$\Gamma^{\mu\mu}_{\mathcal{R}_4}$	$1.50 \pm 1.03 \pm 0.53$	$1.12 \pm 0.89 \pm 0.40$	$1.09 \pm 0.84 \pm 0.39$	$1.40 \pm 1.08 \pm 0.50$
$\phi_{\mathcal{R}_4}$	$31 \pm 51 \pm 20$	$352 \pm 29 \pm 220$	$10 \pm 40 \pm 7$	$22 \pm 44 \pm 15$

structures seen in the dressed cross section typically exceeds those seen in the observed cross section by about 4σ, which is compatible with the increase seen in the data.

The eight solutions summarized in Table I have χ^2 values 135.47, 135.71, 135.76, 135.48, 135.59, 135.95, 135.67, 135.61, respectively, for 121 degrees of freedom. Thus, all of them are acceptable. We choose Solution I as the nominal result of the analysis. The mass and total width of the $S(4220)$ determined from the fit are consistent with those of the $Y(4220)$, $R(4230)$ and $R(4220)$ resonances measured by

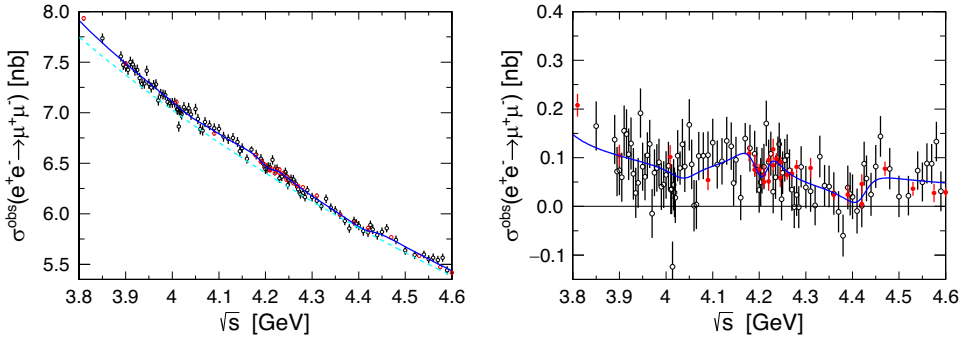

FIG. 2. Measured cross sections for $e^+e^- \to \mu^+\mu^-$ with the fit superimposed. The left plot shows the absolute cross sections, while the right plot shows the cross section after subtraction of both the continuum and $\psi(3686) \to \mu^+\mu^-$ contributions (see text for details).

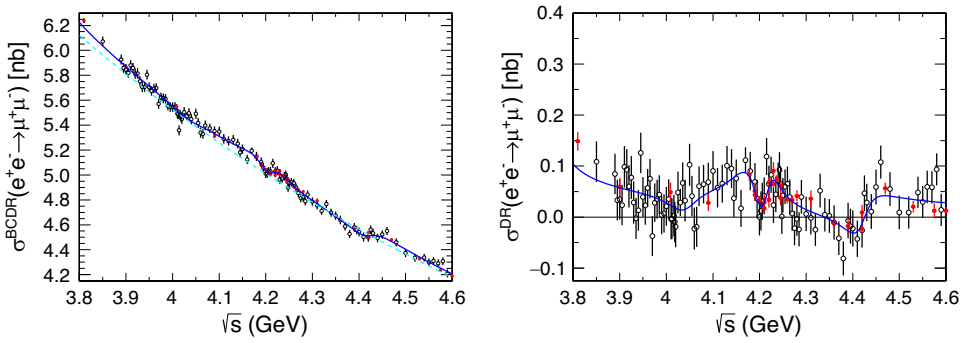

FIG. 3. Corresponding BCDR cross sections for $e^+e^- \to \mu^+\mu^-$ with the fit superimposed. The left plot shows the absolute cross sections, while the right has subtracted both the continuum and $\psi(3686) \to \mu^+\mu^-$ contributions (see text for details).

the BESIII Collaboration [12–14], so these are likely to be the same vector state. With this assumption we obtain the ratios of branching fractions: $\mathcal{B}(S(4220) \to \omega\chi_{c0})/\mathcal{B}(S(4220) \to \mu^+\mu^-) = 54 \pm 77$, $\mathcal{B}(S(4220) \to h_c\pi^+\pi^-)/\mathcal{B}(S(4220) \to \mu^+\mu^-) = 92^{+142}_{-133}$ and $\mathcal{B}(S(4220) \to J/\psi\pi^+\pi^-)/\mathcal{B}(S(4220) \to \mu^+\mu^-) = (32 \pm 46)$ to (266 ± 373), where the uncertainties include both statistical and systematic contributions. These ratios indicate that the branching fraction of the decay $S(4220) \to \mu^+\mu^-$ is typically two orders of magnitude smaller than $S(4220) \to M_{c\bar{c}}\mathrm{X}_{\mathrm{LH}}$ decays.

Our measured muonic widths for the $\psi(4040)$ and $\psi(4415)$ are consistent within ~1.3 times the uncertainties with theoretical expectations for the electronic widths of these states, which are 1.42 and 0.70 keV, respectively [29].

In summary, we have measured the cross section for $e^+e^- \to \mu^+\mu^-$ at c.m. energies from 3.8 to 4.6 GeV. For the first time we have directly measured the muonic widths and branching fractions of $\psi(4040)$, $\psi(4160)$ and $\psi(4415)$, and determined the phases of the decay amplitudes for these three resonances. The relative phases of these three vector states range from (0 ± 40) to (359 ± 183) degrees. In addition, we have found evidence for a structure $S(4220)$ lying near to 4.22 GeV/c^2 with a mass of $M_{S(4220)} = 4216.7 \pm 8.9 \pm 4.1$ MeV/c^2, a total width of $\Gamma^{\mathrm{tot}}_{S(4220)} = 47.2 \pm 22.8 \pm 10.5$ MeV, and a muonic width of $\Gamma^{\mu\mu}_{S(4220)} = 1.53 \pm 1.26 \pm 0.54$ keV, where the first uncertainties are statistical and the second are systematic. The statistical significance of the $S(4220)$ signal is 3.9σ. The analysis of the BCDR cross section of $e^+e^- \to \mu^+\mu^-$ yields a statistical significance of the $S(4220)$ signal of 8.1σ. Although the dimuon branching fractions of the $X_{\mathrm{above\,D\bar{D}}}$ decays are all at the level of $\sim 10^{-5}$, the interference of these decays with the $e^+e^- \to \mu^+\mu^-$ continuum produces a measurable contribution to the cross section, whose shape is sensitive to new states. Therefore the analysis of the $e^+e^- \to \mu^+\mu^-$ cross section in the energy region between 3.73 and 4.8 GeV is a promising way to discover new vector states, complementing the study of the lineshape of cross sections for $e^+e^- \to J/\psi X$, $e^+e^- \to \psi(3686)X$ (X = light hadrons or photons), and $e^+e^- \to$ light hadrons at energies from 3.73 to 4.8 GeV, as well as the study of NOC decays of the $X_{\mathrm{above\,D\bar{D}}}$ states as suggested in Ref. [15].

The BESIII collaboration thanks the staff of BEPCII and the IHEP computing center for their strong support. This work is supported in part by National Key Basic Research Program of China under Contracts No. 2015CB856700, No. 2009CB825204; National Natural Science Foundation of China (NSFC) under Contracts No. 11625523, No. 11635010, No. 11735014, No. 11822506, No. 11835012, No. 11961141012, No. 10935007; the Chinese Academy of Sciences (CAS) Large-Scale Scientific Facility Program; Joint Large-Scale Scientific Facility Funds of the NSFC and CAS under Contracts No. U1532257, No. U1532258, No. U1732263, No. U1832207; CAS Key Research Program of Frontier Sciences under Contracts No. QYZDJ-SSW-SLH003, No. QYZDJ-SSW-SLH040; 100 Talents Program of CAS, CAS Other Research Program under Code No. Y129360; INPAC and Shanghai Key Laboratory for Particle Physics and Cosmology; ERC under Contract No. 758462; German Research Foundation DFG under Contracts No. Collaborative Research Center CRC 1044, FOR 2359; Istituto Nazionale di Fisica Nucleare, Italy; Ministry of Development of Turkey under Contract No. DPT2006K-120470; National Science and Technology fund; STFC (United Kingdom); The Knut and Alice Wallenberg Foundation (Sweden) under Contract No. 2016.0157; The Royal Society, UK under Contracts No. DH140054, No. DH160214; The Swedish Research Council; U.S. Department of Energy under Contracts No. DE-FG02-05ER41374, No. DE-SC-0010118, No. DE-SC-0012069.

[1] F. E. Close and P. R. Page, Phys. Lett. B **578**, 119 (2004).
[2] M. B. Voloshin and L. B. Okun, JETP Lett. **23**, 333 (1976).
[3] N. Brambilla *et al.*, Eur. Phys. J. C **71**, 1534 (2011).
[4] J. Z. Bai *et al.* (BES Collaboration), arXiv:hep-ex/0307028v1; W. G. Li, G. Rong, and D. G. Cassel, in *Proceedings of Tenth International Conference on Hadron Spectroscopy, Aschaffenburg, Germany, 2003* (2003), pp. 495, 592, 937; J. Z. Bai *et al.* (BES Collaboration), HEP & NP **28**, 325 (2004).
[5] J. Z. Bai *et al.* (BES Collaboration), Phys. Lett. B **605**, 63 (2005).
[6] N. E. Adam *et al.* (CLEO Collaboration), Phys. Rev. Lett. **96**, 082004 (2006).
[7] G. Rong, in *Proceedings of the Symposium of 30 Years of BES Physics, Beijing, China* (World Scientific, Singapore, to be published).
[8] S.-K. Choi *et al.* (Belle Collaboration), Phys. Rev. Lett. **91**, 262001 (2003).
[9] B. Aubert *et al.* (*BABAR* Collaboration), Phys. Rev. Lett. **95**, 142001 (2005).
[10] X. L. Wang *et al.* (Belle Collaboration), Phys. Rev. Lett. **99**, 142002 (2007).
[11] M. Ablikim *et al.* (BES Collaboration), Phys. Rev. Lett. **101**, 102004 (2008).
[12] M. Ablikim *et al.* (BESIII Collaboration), Phys. Rev. Lett. **118**, 092001 (2017).
[13] M. Ablikim *et al.* (BESIII Collaboration), Phys. Rev. Lett. **114**, 092003 (2015).
[14] M. Ablikim *et al.* (BESIII Collaboration), Phys. Rev. Lett. **118**, 092002 (2017).
[15] G. Rong, Chin. Phys. C **34**, 788 (2010).
[16] M. Ablikim *et al.* (BESIII Collaboration), Chin. Phys. C **41**, 063001 (2017); **39**, 093001 (2015).
[17] M. Ablikim *et al.* (BESIII Collaboration), Chin. Phys. C **40**, 063001 (2016).
[18] M. Ablikim *et al.* (BESIII Collaboration), Nucl. Instrum. Methods Phys. Res., Sect. A **614**, 345 (2010).
[19] S. Agostinelli *et al.* (GEANT4 Collaboration), Nucl. Instrum. Methods Phys. Res., Sect. A **506**, 250 (2003).
[20] G. Balossini, C. M. Carloni Calame, G. Montagna, O. Nicrosini, and F. Piccinini, Nucl. Phys. **B758**, 227 (2006); G. Balossini, C. Bignamini, C. M. Carloni Calame, G. Montagna, O. Nicrosini, and F. Piccinini, Phys. Lett. B **663**, 209 (2008).
[21] S. Jadach, B. F. L. Ward, and Z. Was, Comput. Phys. Commun. **130**, 260 (2000).
[22] T. K. Pedlar *et al.* (CLEO Collaboration), Phys. Rev. Lett. **95**, 261803 (2005).
[23] M. Ablikim *et al.* (BES Collaboration), Phys. Lett. B **641**, 145 (2006).
[24] M. Ablikim *et al.* (BES Collaboration), Phys. Rev. Lett. **97**, 262001 (2006).
[25] E. A. Kuraev and V. S. Fadin, Yad. Fiz. **41**, 377 (1985) [Sov. J. Nucl. Phys. **41**, 466 (1985)].
[26] M. Botje, J. Phys. G **28**, 779 (2002).
[27] M. Tanabashi *et al.*, Phys. Rev. D **98**, 030001 (2018).
[28] M. Ablikim *et al.* (BES Collaboration), Phys. Rev. Lett. **97**, 121801 (2006).
[29] B. Q. Li and K. T. Chao, Phys. Rev. D **79**, 094004 (2009).